

000 LATENTS-INV: ROBUST SEMANTIC WATERMARK WITH 001 KEY-ASSISTED RECOVERY FOR DIFFUSION MODELS 002 003 004

005 **Anonymous authors**

006 Paper under double-blind review

007 008 ABSTRACT 009 010

011 Semantic watermarking provides imperceptible identity traceability for diffusion-
012 generated images, enabling model copyright protection and image source verifi-
013 cation. However, existing semantic watermarking methods based on initial latent
014 noise render the protected image vulnerable to adversarial latent-space manipula-
015 tions, such as black-box forgery via proxy models and watermark-pattern-removal
016 attacks that exploit statistical regularities. In this paper, we propose a robust water-
017 marking framework resilient diverse adversarial manipulation attack. Specifically,
018 we design a fully reversible, flow-based codec with dual encoding paths, allowing
019 plug-and-play integration into the diffusion generation process across architec-
020 tures (UNet and MMDiT). The dual-output network encodes watermark informa-
021 tion into both the carrier image and the owner’s secret key, enabling recovery of
022 removal attacked watermark via key-assisted reconstruction. To guarantee verifi-
023 cation reliability without excessive reliance on the key while retaining the ability
024 to detect forged watermarked images, we propose a joint-training strategy that
025 leverages negative-sample pairs under both accuracy and fidelity constraints. Fur-
026 thermore, we introduce an Euler-based enhanced solver for the effective inversion
027 in rectified flow models, which improves the accuracy of watermark information
028 recovered. Experimental results show that our method achieves superior robust-
029 ness under various attacks while maintaining high visual quality across diverse
030 models.

031 032 1 INTRODUCTION

033 Digital watermarking helps improve security in content creation based on strong cross-modal vision
034 models(Xian et al., 2024; Song et al., 2024; Lei et al., 2024; Zhang et al., 2024b). Individuals
035 with different backgrounds can train personalized models based on their own needs, resulting in
036 various models that generate content of quality similar to human-created content(Rombach et al.,
037 2022; Ho et al., 2020; Xu et al., 2024).. However, this open approach to model customization brings
038 trust issues, such as model theft, copyright disputes, and the generation of fake contentZhang et al.
039 (2024c). Watermark information can not only be used to protect model copyright, which is valuable
040 intellectual property from large-scale training. But also to embed traceable data into the model’s
041 outputs(Bao et al., 2024; Pan et al., 2024b). This makes it possible to check the source of generated
042 content(Min et al., 2024; Feng et al., 2024; Chen et al., 2024), helping to identify fake, false, or
043 illegally used outputs, and ensuring that generated results are secure, reliable, and trustworthy.

044 For generative models of visual content, watermark information can be embedded by marking the
045 model’s outputs with a secret message(Chen et al., 2024; Pan et al., 2024b; Trias et al., 2024). Cur-
046 rently, the main watermarking methods fall into two categories: post-processing and in-processing
047 approaches. Post-processing is similar to traditional image watermarking. It steganographically
048 embeds information into the output after the model generates the data. However, this approach is
049 easily affected by image-level detection and attacksLiu et al. (2024). In contrast, most current water-
050 marking methods for diffusion models embed verifiable information during the generation process,
051 at specific stages of image creation. These methods include fine-tuning parts of the model(Rezaei
052 et al., 2024; Hu et al., 2024a) and watermarking the initial noise before the denoising process(Wen
053 et al., 2023; Ci et al., 2024; Yang et al., 2024b).

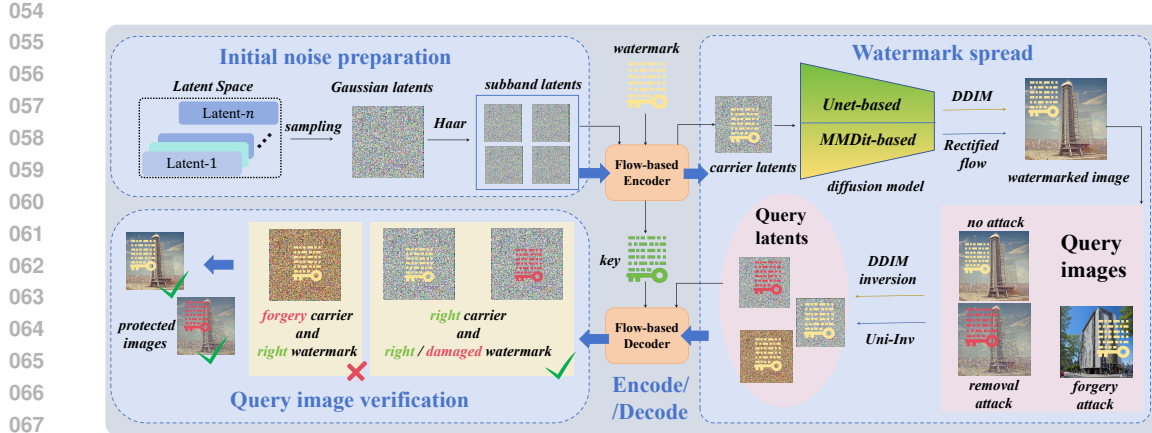


Figure 1: Framework of the proposed method system. Latents-Inv uses the sampled and transformed sub-band signals as the watermark carrier. During spreading, the watermark information may be partially removed from the denoised image or forged on an attacker’s image. In the verification phase, forgery attacks do not cause confusion, and removal attacks do not prevent ownership identification.

The first method is designed for specific model architectures, it has poor generalization—watermarking methods for UNet-based models often do not transfer well to MMDiT-based models. Therefore, in this paper, we propose Latents-Inv. This method still embeds watermark information into the latent representations at the beginning of generation for various models, as shown in Figure 1. This approach is theoretically convenient for achieving plug-and-play compatibility across different models. However, in practice, extracting semantic watermarks relies on accurate inversion and reversible distribution transformation. Due to differences in latent space dimensions and denoising processes across models, current watermarking approaches are not fully compatible, often leading to significant drops in robustness and generation quality Umrajkar & Singh (2025). For UNet-based diffusion models, watermarking typically uses mature inversion methods like DDIM or DPM-Solver, which are based on ODE solvers Zhao et al. (2022). In contrast, more advanced models with MMDiT architecture use a Rectified Flow-based denoising process. This is first-order Euler-like method and requires iterative approach to reduce inversion errors Rout et al. (2024). To address the precision issue, our method predicts the backward-step noise from the forward-step predictions and then uses this estimate to refine the forward prediction, as detailed in 3.4.

Moreover, although several semantic watermarking methods in the noise space have been proposed, their robustness has been challenged by various watermark attacks. For generated images that require verification, traditional image transformations—such as cropping and noising—can unintentionally or deliberately damage the watermark by altering the pixel values of the image. Modern attacks, however, focus more on breaking the watermark pattern while preserving image quality, aiming to either remove or forge watermark information and thus undermine its credibility Yang et al. (2024a). Existing semantic watermarking methods show poor robustness against proxy-model-based deep perturbation attacks on single images, where watermarks can be easily erased Müller et al. (2025). Furthermore, when an attacker has access to a large number of watermarked images sharing the same pattern, there is a risk that the watermark pattern can be statistically analyzed and stolen using a proxy model, enabling watermark removal and forgery Pan et al. (2024a).

Therefore, Latents-Inv primarily addresses the robustness issue. Its core idea is to use the owner’s key to recover the damaged parts of a watermark when the carrier image is inevitably attacked, enabling fine-grained verification with sufficient accuracy. We employ a flow-based model with a bidirectional structure to reversibly embed and accurately extract watermark information. This model uses dual-channel outputs to distribute the watermark: one channel contains the initial latents with the embedded watermark, and the other contains the copyright owner’s key also embedded with watermark information. To ensure that watermark verification does not overly depend on the key, we apply a joint-training strategy during training that utilizes negative sample pairs under both accuracy and fidelity constraints. Additionally, we train a coarse-grained decoder with the same architecture but different parameters to enable watermark extraction from images even without the key, ensuring

108 full utilization of the carrier’s frequency-domain information capacity during the watermark encoding
 109 phase.

110 In summary, our method minimizes perturbation to the latent representations at the early generation
 111 stage, ensuring that the embedded watermark remains highly imperceptible in the final generated im-
 112 ages. Experimental results show that current statistical attack methods cannot detect or distinguish
 113 the watermark pattern in Latents-Inv. Moreover, our method includes a robust watermark extrac-
 114 tion system that maintains strong ownership identification capability even when the watermark in
 115 the carrier image is disturbed by attackers. Furthermore, our approach achieves lossless watermark-
 116 ing in diffusion models—tested on both advanced first-order Euler-based models and DDIM-based
 117 diffusion models, it achieves consistent and strong watermarking performance.

119 2 RELATED WORK

120 2.1 WATERMARK METHOD

123 Embedding watermark information into data as traceable metadata is highly beneficial for source
 124 verification and copyright protection. Traditional image watermarking techniques directly embed
 125 invisible watermarks into the spatial or transform domain of the target image, serving as a post-
 126 processing steganographic method for traceability(Liang et al., 2024; Müller et al., 2025; Liu et al.,
 127 2024). However, with the development and maturity of AI generative models, watermarking meth-
 128 ods are increasingly integrated into the image generation process itselfArabi et al. (2025). This not
 129 only improves the robustness of low-perturbation watermarks but also enables attribution of gen-
 130 erated images based on the specific watermarking method used by a model, thus protecting both
 131 content and model ownership(Saberi et al., 2023; Liang et al., 2024). In-processing approaches vary
 132 across different generative models, but the main strategies fall into two categories: one fine-tunes
 133 part of the model structure to embed watermark information during image generationFeng et al.
 134 (2024); the other embeds the watermark at the initial noise sampling stage of diffusion models,
 135 which reduces computational overhead(Yang et al., 2024b; Ci et al., 2024; Arabi et al., 2024).

136 2.2 ANTI-WATERMARK METHOD

138 Robustness against attacks remains a key challenge for modern semantic watermarking. Early water-
 139 mark removal methods relied on simple image transformations—such as cropping, noise addition,
 140 and rotation—which physically alter the image to disrupt invisible watermarks embedded in the
 141 spatial or transform domain.Liang et al. (2024) However, with advances in neural networks and
 142 deep learning, such post-processed perturbative watermarks can be easily detected and removed by
 143 deep modelsJiang et al. (2023). Meanwhile, existing in-processing watermarking methods embed
 144 information during generation, but they often rely on fixed mathematical patterns in the initial noisy
 145 latent, leading to consistent image distributions. This makes the watermark vulnerable to statistical
 146 analysis(Zhang et al., 2024a; Yang et al., 2024a) or proxy models(Hu et al., 2024b; Müller et al.,
 147 2025) that can learn the embedding pattern, enabling watermark removal or forgery. In addition, wa-
 148 termarking methods based on fine-tuning parts of the generator are limited by fixed model modules
 149 and can be erased using regeneration attacks on diffusion models(Zhao et al., 2024; Liu et al., 2024).
 150 These vulnerabilities show that current watermarking approaches still lack sufficient robustness.

151 2.3 DIFFUSION MODELS

153 Besides security concerns, the lack of cross-architecture generalizability is another key limitation
 154 of existing watermarking methods. Most watermarking proposals are designed for older generation
 155 models—particularly diffusion models based on the UNet architecture and the DDIM sampling pro-
 156 cessMokady et al. (2023). DDIM approximates the original SDE process of DDPM—which is based
 157 on a Markov chain—as an ODE-solving processZhao et al. (2022). Although this simplification in-
 158 troduces some approximation error, it makes the parameters at any noising or denoising timestep
 159 explicitly known, enabling efficient inversion from the generated image back to its corresponding
 160 initial noise. And the forward Euler method for denoising follows an ODE-solving procedure, but
 161 the backward Euler method is implicit. In the inversion process, this manifests as a mismatch be-
 162 tween the prompt embedding vectors in the forward and backward passes, necessitating an iterative

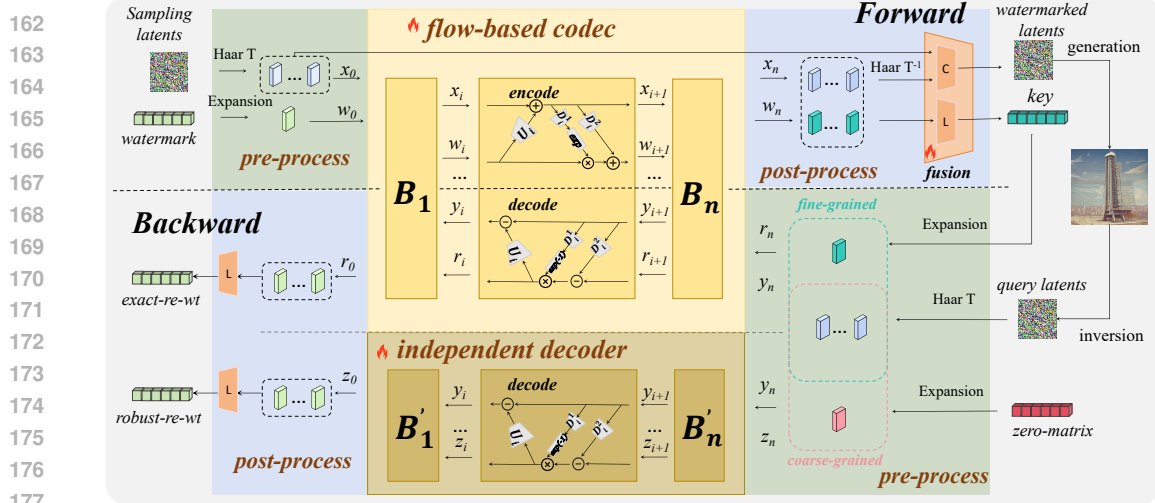


Figure 2: The core watermark encoding and decoding structure of Latents-Inv, encompassing pre-processing, encode-decode, and post-processing stages. Pre-processing primarily employs mathematical techniques for channel expansion, thereby increasing the embeddable regions for watermark information. The flow-based encoder manages the forward process, sharing model weights with the corresponding flow-based decoder during the reverse process, while maintaining an identical architecture to that of the independent decoder. Post-processing focuses on feature fusion, ensuring dimensional consistency between inputs and outputs, as well as preserving the distribution characteristics of the latents.

solver to achieve consistency. As a result, watermarking methods that rely on fine-tuning model components fail to achieve consistent embedding and protection performance when applied to newer models based on the MMDiT architecture and rectifield-flow method Liu et al. (2022). Similarly, approaches that embed watermarks in the initial noise suffer significant performance degradation due to architectural and procedural differences in the generation pipeline Umrajkar & Singh (2025). Specifically, models using the rectifield-flow method no longer employ only ODE-based sampling like DDIM for noising or denoising. This necessitates a new inversion method to reliably map generated images back to their corresponding initial noise (Wang et al., 2024; Deng et al., 2024; Rout et al., 2024; Jiao et al., 2025), ensuring stable watermark embedding and extraction within the initial noise space.

3 METHOD

3.1 OVERVIEW

As shown in Figure 2, during encoding, the core of our method is using a flow-based model to embed watermark information into two outputs: the carrier latents and a owner’s key. After generation and inversion, Latents-Inv should verify the query latents. In the extraction phase, fine-grained and high-precision watermark recovery is achieved with the aid of the key, while a key-free coarse-grained decoder assesses the level of watermark corruption in the carrier, helping to verify the legitimacy of the fine-grained extraction result and preventing false acceptance of forged or unauthorized content. Next, we present a detailed description of the codec operational mechanism and training strategy, along with the Uni-inv inversion method tailored for MMDiT-based diffusion models.

3.2 LATENTS PROCESSING AND FLOW-BASED CODEC

The flow-based model is inherently reversible: for every forward encoding function f_θ , there exists a corresponding backward function f_θ^{-1} . This one-to-one invertibility naturally aligns with the watermarking pipeline, where embedding and extraction are symmetric processes. However, before any forward or backward pass through the flow model, as illustrated in Figure 2, the input must go through pre-processing and post-processing.

216 During pre-processing, Latents-Inv will transform the latent noise into four frequency domains
 217 through two-dimensional HARR transformation. Embedding the watermark information multiple
 218 times into the HARR-transformed information can better utilize the channel capacity than embed-
 219 ding it once in the spatial domain. And watermark can be more robust without affecting the qual-
 220 ity(Wen et al., 2023; Kassis & Hengartner, 2025).

221 In the embedding stage, Latents-Inv accepts the watermark information \mathbf{m}_0 and the carrier infor-
 222 mation \mathbf{x}_0 . And in each invertible block, the model performs additive affine transformations to
 223 gradually blend the watermark with the carrier image. Finally, it outputs the watermarked carrier \mathbf{x}_n
 224 and the owner's key \mathbf{m}_n . Here is the invertible block:

$$x_{i+1} = x_i + U_i(m_i) \quad (1)$$

$$m_{i+1} = m_i \otimes \exp(D_i^1(x_{i+1})) + D_i^2(x_{i+1}) \quad (2)$$

225 where U_i denotes the update network, D_i^1, D_i^2 are diffusion sub-networks, and \otimes indicates element-
 226 wise multiplication. In the extraction stage, we input the key \mathbf{r}_n and the watermark carrier \mathbf{y}_n
 227 through backward input, and extract the watermark information by performing the same parameter
 228 convolution and reverse coupling of the carrier and key feature information precisely. The corre-
 229 sponding backward propagation of the extraction process is formulated as:

$$m'_i = (m_{i+1} - D_i^2(x'_{i+1})) \otimes \exp(-D_i^1(x'_{i+1})) \quad (3)$$

$$x'_i = x'_{i+1} - U_i(m'_i) \quad (4)$$

230 At the same time, we also use a trained coarse-grained watermark decoder with the same structure,
 231 inputting an empty matrix \mathbf{z}_n and the watermark carrier \mathbf{y}_n , and directly extracting the watermark
 232 information from the carrier. Coarse-grained occurs before fine-grained extraction, it can ensure the
 233 validity of the carrier information and ensure that fine-grained extraction does not overly rely on the
 234 redundant residual watermark information in the key.

235 Post-processing ensures consistent data dimensions and helps preserve output image quality. In the
 236 whole process, the key is processed by a fully connected (fc) layer to match the same dimension
 237 as the original watermark. For carrier latents, Latents-Inv concatenates the clean and watermarked
 238 frequency-domain signals across the four bands along the channel dimension, followed by a 1×1
 239 convolution. This ensures that the initial noise fed into the diffusion model contains the watermark
 240 and better matches the desired noise distribution.

241 3.3 WATERMARK ROBUSTNESS PROTECTION

242 To address the issue of robustness, our method hides the watermark information through an invertible
 243 latent watermark encoder-decoder in two parts: the released carrier image and the private key owned
 244 by the image owner. Since the watermark information associated with the private key remains intact,
 245 our method is inherently robust against attacks that attempt to corrupt the watermark in the carrier.
 246 To ensure reliable verification, however, it is essential to have sufficient discriminative capability
 247 over the distribution of latents paired with the key.

248 First, we evaluate watermark embedding and extraction under noise-free conditions, which serves
 249 as the fundamental criterion for assessing embedding and decoding accuracy. Unlike prior semantic
 250 watermarking methods, Latents-Inv preserves the distribution of the discretized latent noise as much
 251 as possible during modification, thereby maintaining content consistency of the generated images
 252 before and after watermark embedding. Our joint training strategy for image generation quality and
 253 accuracy is as follows:

$$\mathcal{L}_\theta = \mathbb{E}_{m_0, \mathbf{x}_0} \left[\|\mathbf{x}_0 - \pi_{\mathbf{x}} \circ f_\theta(m_0, \mathbf{x}_0)\|^2 + \|m_0 - \pi_m \circ f_\theta^{-1} \circ f_\theta(m_0, \mathbf{x}_0)\|^2 \right] \quad (5)$$

254 where $\pi_{\mathbf{x}}(\mathbf{x}, m) = \mathbf{x}$ and $\pi_m(\mathbf{x}, m) = m$ are the natural projections. We avoid using KL divergence
 255 as the distribution loss because it may not sufficiently constrain the L_2 distance between the initial
 256 latents before and after watermark embedding, potentially leading to perceptible distortions in the
 257 generated image.

258 To enhance robustness against watermark destruction attacks, we leverage the multi-band capacity
 259 of the initial latent noise and employ a fully reversible, dual-end flow-based architecture. To prevent

270 the model from over-relying on the key for watermark encoding—thus underutilizing the latent
 271 space—we introduce a coarse-grained structural decoder. It takes a zero matrix and the carrier
 272 noise as input and reconstructs the initial watermark, promoting watermark embedding in the latent
 273 channel while preserving the integrity of the carrier image. The corresponding loss is:
 274

$$\mathcal{L}_{\theta'} = \mathbb{E}_{m_0, \mathbf{x}_0, z_0} \|m_0 - \pi_m \circ f_{\theta'}^{-1} \circ (f_{\theta}(m_0, \mathbf{x}_0), z_0)\|^2 \quad (6)$$

277 For watermark forgery through the published carrier image, we introduce negative samples pairs
 278 through regularization penalties, so that the trained flow-based model pays more attention to the
 279 noisy latents with key-paired watermark information during decoding. We employ the BCE loss as
 280 a metric to measure the wrong classification rate on negative sample pairs, and introduce a penalty
 281 term to prevent overfitting:
 282

$$\mathcal{L}_{bce} = BCE(m_0, \pi_m \circ f_{\theta}(m_0, \mathbf{x}_0)) \quad (7)$$

$$P_{\text{neg}} = \max(0, 0.6930 - (\mathcal{L}_{bce} - \mathcal{L}_{\theta'})) \quad (8)$$

285 The penalty threshold is set to 0.6930, which corresponds to the BCE loss of a random guess on a
 286 balanced binary watermark sequence. At the same time, negative sample pairs prevent the decoder
 287 from relying too much on the key, ensuring the latent noise is also used for watermark extraction.
 288 This avoids false detection when arbitrary noise is paired with a key.
 289

290 In brief, to balance watermark embedding between the carrier and the key, we combine coarse- and
 291 fine-grained decoding with negative-sample training. The overall training loss with the correspond-
 292 ing weight coefficients λ_1 , λ_2 and λ_3 is:
 293

$$\mathcal{L}_{\text{total}} = \lambda_1 \mathcal{L}_{\theta} + \lambda_2 \mathcal{L}_{\theta'} + \lambda_3 P_{\text{neg}}. \quad (9)$$

294 3.4 INVERSION METHOD IN RECTIFIED-FLOW DIFFUSION MODEL

295 Diffusion-based generative models aim to map initial noise samples drawn from a Gaussian distri-
 296 bution to realistic data distributions. The inversion process seeks to reconstruct the reverse diffusion
 297 trajectory in order to recover the initial latent noise corresponding to a given generated image—a
 298 critical step for accurately extracting watermarks embedded via latent noise modulation. However,
 299 recent models such as SD3 and FLUX adopt Rectified Flow formulations rather than DDIM-style
 300 ODE solvers:
 301

$$Z_{t_{i-1}} = Z_{t_i} + (t_{i-1} - t_i)v_{\theta}(Z_{t_i}, t_i) \quad (10)$$

302 where $Z_{t_{i-1}}$ denotes the latents at timestep t_i , and Z_{t_i} is the latents from the previous step. The term
 303 $t_{i-1} - t_i$ represents the time step size, and $v_{\theta}(Z_{t_i}, t_i)$ is the velocity network that predicts the flow
 304 direction at t_i . This explicit forward Euler update simulates the continuous transformation from data
 305 to Gaussian noise in Rectified Flow diffusion models. So, the inversion process may clear:
 306

$$Z_{t_i} = Z_{t_{i-1}} - (t_{i-1} - t_i)v_{\theta}(Z_{t_i}, t_i). \quad (11)$$

307 The variable $v_{\theta}(Z_{t_i}, t_i)$ is unknown in the backward Euler method. Consequently, the inversion
 308 method cannot be straightforwardly derived from the forward process, due to the non-ODE formu-
 309 lation and implicit backward dynamics of modern flow-based models. Therefore, in the experiment,
 310 we adopted the precise inversion method of Uni-InvJiao et al. (2025), which reverses the previous
 311 value of hidden Euler approach back to the next value. Given the velocity function v_0 , initial image
 312 $Z_0 \sim \pi_0$, and time steps $t = \{t_0, \dots, t_N\}$ where $t_0 = 0$ and $t_N = 1$, the Uni-Inv (Euler) algorithm
 313 updates are defined as follows:
 314

315 Initial conditions:
 316

$$\hat{v}_0 = v_0(Z_0, t_0) \quad (12)$$

$$\hat{Z}_{t_0} = Z_0 \quad (13)$$

317 For $i = 1$ to N :

$$\bar{Z}_{t_i} = \hat{Z}_{t_{i-1}} - (t_{i-1} - t_i)\hat{v}_{i-1} \quad (14)$$

$$\hat{v}_i = v_{\theta}(\bar{Z}_{t_i}, t_i) \quad (15)$$

$$\hat{Z}_{t_i} = \bar{Z}_{t_{i-1}} - (t_{i-1} - t_i)\hat{v}_i \quad (16)$$

The final output we want is \hat{Z}_1 . Uni-Inv is fundamentally an iterative generation method designed for the backward Euler ODE solver, also known as the predictor-corrector method—a classical and effective approach in numerical analysis for solving differential equations. The theoretical error is $\mathcal{O}(\Delta t_i^3)$, where $\Delta t_i = t_i - t_{i-1}$, and the proof is shown in the appendix. It transitions to the high-noise step first, estimates the velocity by simulating a denoising process. Then it returns to the original low-noise step and performs inversion using the latest “denoising-like” velocity. Intuitively, because the initial and end noise distributions are similar, the parallel noise distribution errors on the same time step with the same length will be smaller.

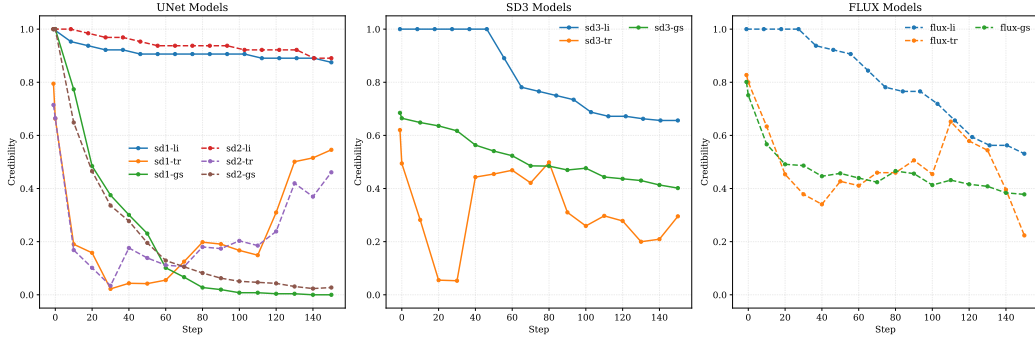


Figure 3: Robustness of semantic watermarking methods under surrogate-model-based removal attacks across different diffusion architectures.

4 EXPERIMENTS

4.1 EXPERIMENTAL SETUP

Datasets. In our experiments, we use a combination of real and synthetic images. We randomly select 5,000 real images from COCO2017 as clean, unwatermarked samples to serve as the reference pattern in detection. We generate 19,000 clean images and 1,000 watermarked images with SD3, where 10% of the watermarked set is used as training data. All images are generated from prompts in the Stable-Diffusion-Prompt dataset and are also used to evaluate detection performance.

Diffusion Models. We evaluate across four diffusion models: SD1.5 as a representative UNet-based architecture, and SD3.medium and FLUX1.dev for testing under MMDiT and rectified flow (RF) generation frameworks. For black-box forgery and removal attacks Müller et al. (2025), we adopt SD2.1-baseRombach et al. (2022) as the surrogate model.

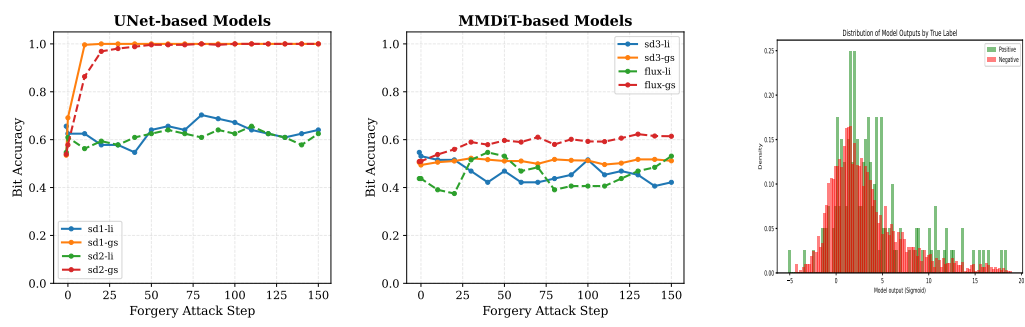


Figure 4: Robustness of semantic watermarking methods under surrogate-model-based forgery attacks across different diffusion architectures.

Figure 5: Distribution of images after statistical analysis detection.

Watermarking and Adversarial Methods. We compare with semantic watermarking methods that embed information in the initial latent noise, focusing on those transferable from UNet to MMDiT architectures. We select Tring-Ring (TR)Wen et al. (2023) and Gaussian Shaping (GS)Yang et al. (2024b) as baselines. To assess robustness, we consider two attack paradigms: (i) single-image

latent inversion attacks that perturb initial latents Müller et al. (2025), and (ii) statistical detection methods that analyze patterns across large collections of watermarked images Yang et al. (2024a); Pan et al. (2024a). The former can perform threatening watermark removal and forgery attacks and the latter can effectively distinguish the distribution of watermarked images from clean images.

Evaluation Metrics. We use **bit accuracy** as the primary metric for GS and Latents-Inv watermark extraction robustness. We measure TR watermark extraction robustness with the p-value, which gives the probability that the observed watermark would appear by random chance—smaller values indicate stronger evidence of the true watermark. And for monotonicity consistency, we use 1-p-value for comparison.

Table 1: Comparison of Different Methods

Method	Model	Clean	Crop	Noise	Bright	Removal	Forgery	Avg ↑
Tree-Ring	SD1.5	0.963	0.067	0.522	0.631	0.546	0.000	0.455
	SD2.1	0.978	0.079	0.544	0.664	0.461	0.000	0.454
	SD3.0	0.694	0.032	0.312	0.353	0.295	0.005	0.282
	FLUX.1	0.722	0.041	0.383	0.419	0.223	0.017	0.301
Gaussian-Shading	SD1.5	1.000	0.847	0.693	0.864	0.003	0.000	0.568
	SD2.1	1.000	0.848	0.715	0.825	0.027	0.000	0.569
	SD3.0	0.787	0.648	0.576	0.626	0.402	0.489	0.588
	FLUX.1	0.804	0.683	0.608	0.705	0.322	0.386	0.585
Latents-Inv (Ours)	SD1.5	1.000	0.821	0.724	0.869	0.906	0.359	0.777
	SD2.1	1.000	0.831	0.745	0.872	0.856	0.375	0.780
	SD3.0	1.000	0.812	0.728	0.822	0.656	0.593	0.769
	FLUX.1	0.984	0.804	0.687	0.794	0.781	0.532	0.764

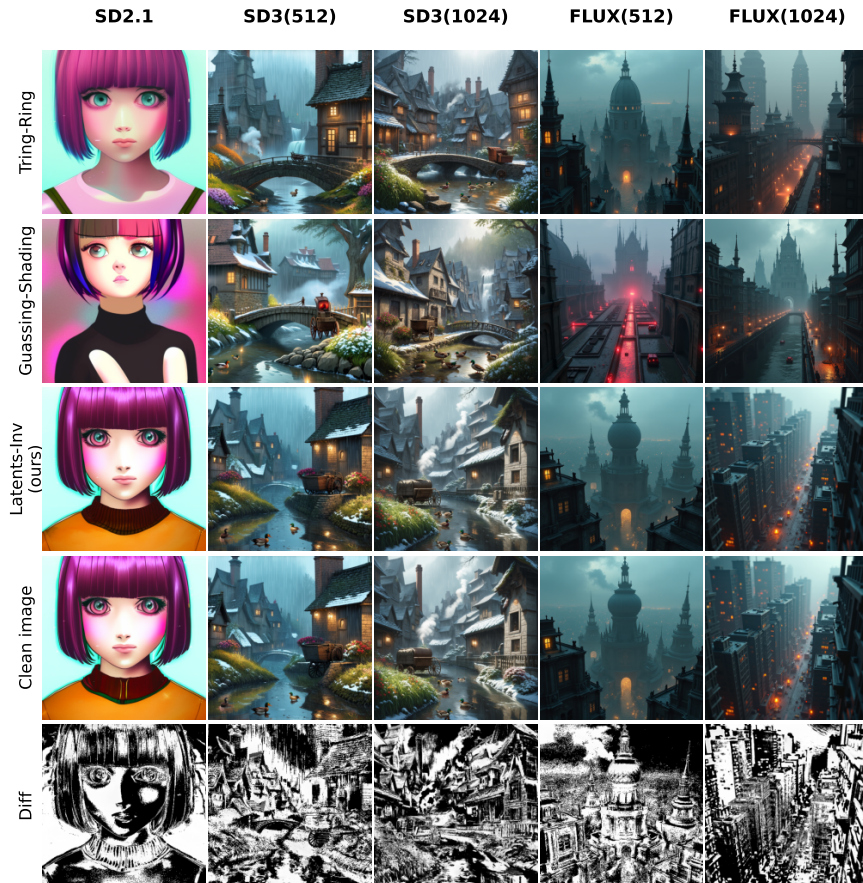
4.2 EXPERIMENTAL RESULTS

Watermark Robustness Performance of Latents-Inv: Table 1 summarizes robustness evaluation results under both traditional image distortions and black-box watermark removal attacks using the SD2.1-based surrogate model. Under conventional attacks, semantic watermarking methods based on initial latent noise generally show reliable performance. Our method achieves competitive or superior bit accuracy across most cases. Notably, while Latents-Inv performs slightly worse than GS under cropping on UNet-based models, our approach maintains consistent robustness. Even when the latent channel dimension increases from 4 to 16, our method preserves the highest detection rate, demonstrating minimal interference during model transfer and achieving over 98% accuracy on both SD3 and FLUX1.dev.

Under black-box attacks via latent space manipulation, our method shows strong resilience. As shown in Figure 3, with increasing optimization steps in the surrogate model, all semantic watermarks suffer some degradation. GS degrades rapidly on U-Net-based models, whereas our method maintains over 85% accuracy, showing stable robustness. On MMDiT models, our watermark remains robust in early stages and degrades gracefully, still outperforming baselines. Interestingly, TR, which embeds watermark in a ring-like structure similar to physical patterns, exhibits oscillating behavior under iterative perturbation—consistent with the nature of the optimization-based attack. A detailed analysis is provided in the Appendix. Figure 4 shows results under black-box forgery attacks using a surrogate model, where the ring-based non-bit-embedding watermark (TR) is excluded for clarity. On UNet-based models, our method significantly outperforms GS. On MMDiT models, our approach also achieves better robustness, though the performance gap is smaller. Notably, due to architectural differences and limitations of the surrogate model, such forgery attacks struggle to effectively manipulate semantic watermarks across different model architectures—indicating limited cross-structure transferability of current latent space manipulation techniques.

Watermark Visual Performance of Latents-Inv: Figure 6 shows images generated by different diffusion models using various initial latent codes under the same prompt. SD3 and FLUX generate images at resolutions of 512×512 and 1024×1024 , respectively, requiring latents of different dimensions—enabling us to evaluate watermarking under varying latent spaces. Visually, our method

432 produces results most consistent with the clean (unwatermarked) images, thanks to a distribution-
 433 preserving loss used during embedding. Figure 5 also presents results from a black-box statistical
 434 detection test on Latents-Inv. Negative indicates watermarked images, while Positive represents
 435 clean images. The detector fails to reliably distinguish between watermarked and unwatermarked
 436 images, indicating that our embedded latents closely match the distribution of clean ones. This
 437 explains the high visual fidelity of the generated outputs. In the last row of Figure 6, we show the
 438 pixel-wise difference between images generated from watermarked and clean latents. The residual
 439 signal is widespread across the entire image space, demonstrating that Latents-Inv embeds rich, spa-
 440 tially distributed watermark information. This full-spatial presence of watermark traces contributes
 441 significantly to its robustness—ensuring detectable signals remain even after partial corruption or
 442 attacks.



471
 472 Figure 6: Comparison of semantic watermark images generated by different models at various res-
 473 olutions. The first three rows represent watermarked images, the fourth row shows clean (unwa-
 474 termarked) images for reference, and the last row highlights watermark artifacts produced by the
 475 Latents-Inv method.

478 5 CONCLUSION

480 In this work, we propose Latents-Inv, a semantic watermarking method for diffusion models that
 481 embeds invertible watermarks into the initial latent space. By employing a joint-training strategy
 482 that leverages negative-sample pairs under both accuracy and fidelity constraint for a flow-based
 483 codec. Our method achieves high visual fidelity and strong robustness across diverse architectures,
 484 including UNet and MMDiT. Extensive experiments show that Latents-Inv outperforms existing
 485 methods under both traditional distortions and black-box removal/forgery attacks, demonstrating
 superior transferability and resilience.

486 REFERENCES
487

488 Kasra Arabi, Benjamin Feuer, R Teal Witter, Chinmay Hegde, and Niv Cohen. Hidden in the noise:
489 Two-stage robust watermarking for images. *arXiv preprint arXiv:2412.04653*, 2024.

490 Kasra Arabi, R Teal Witter, Chinmay Hegde, and Niv Cohen. Seal: Semantic aware image water-
491 marking. *arXiv preprint arXiv:2503.12172*, 2025.

492

493 Erjin Bao, Ching-Chun Chang, Hanrui Wang, and Isao Echizen. Purification-agnostic proxy learn-
494 ing for agentic copyright watermarking against adversarial evidence forgery. *arXiv e-prints*, pp.
495 arXiv–2409, 2024.

496

497 Yuzhang Chen, Jiangnan Zhu, Yujie Gu, Minoru Kuribayashi, and Kouichi Sakurai. Freemark:
498 A non-invasive white-box watermarking for deep neural networks. *arXiv preprint
arXiv:2409.09996*, 2024.

499

500 Hai Ci, Pei Yang, Yiren Song, and Mike Zheng Shou. Ringid: Rethinking tree-ring watermarking
501 for enhanced multi-key identification. In *European Conference on Computer Vision*, pp. 338–354.
502 Springer, 2024.

503

504 Yingying Deng, Xiangyu He, Changwang Mei, Peisong Wang, and Fan Tang. Fireflow: Fast inver-
505 sion of rectified flow for image semantic editing. *arXiv preprint arXiv:2412.07517*, 2024.

506

507 Weitao Feng, Wenbo Zhou, Jiyan He, Jie Zhang, Tianyi Wei, Guanlin Li, Tianwei Zhang, Weiming
508 Zhang, and Nenghai Yu. Aqualora: Toward white-box protection for customized stable diffusion
509 models via watermark lora. *arXiv preprint arXiv:2405.11135*, 2024.

510

511 Jonathan Ho, Ajay Jain, and Pieter Abbeel. Denoising diffusion probabilistic models. *Advances in
neural information processing systems*, 33:6840–6851, 2020.

512

513 Runyi Hu, Jie Zhang, Yiming Li, Jiwei Li, Qing Guo, Han Qiu, and Tianwei Zhang. Supermark:
514 Robust and training-free image watermarking via diffusion-based super-resolution. *arXiv preprint
arXiv:2412.10049*, 2024a.

515

516 Yuepeng Hu, Zhengyuan Jiang, Moyang Guo, and Neil Zhenqiang Gong. A transfer attack to image
517 watermarks. *arXiv preprint arXiv:2403.15365*, 2024b.

518

519 Zhengyuan Jiang, Jinghuai Zhang, and Neil Zhenqiang Gong. Evading watermark based detection
520 of ai-generated content. In *Proceedings of the 2023 ACM SIGSAC Conference on Computer and
Communications Security*, pp. 1168–1181, 2023.

521

522 Guanlong Jiao, Biqing Huang, Kuan-Chieh Wang, and Renjie Liao. Unedit-flow: Unleashing in-
523 version and editing in the era of flow models. *arXiv preprint arXiv:2504.13109*, 2025.

524

525 Andre Kassis and Urs Hengartner. Unmarker: A universal attack on defensive image watermarking.
526 In *2025 IEEE Symposium on Security and Privacy (SP)*, pp. 2602–2620. IEEE, 2025.

527

528 Liangqi Lei, Keke Gai, Jing Yu, Liehuang Zhu, and Qi Wu. Conceptwm: A diffusion model water-
529 mark for concept protection. *arXiv preprint arXiv:2411.11688*, 2024.

530

531 Yuqing Liang, Jiancheng Xiao, Wensheng Gan, and Philip S Yu. Watermarking techniques for large
532 language models: A survey. *arXiv preprint arXiv:2409.00089*, 2024.

533

534 Xingchao Liu, Chengyue Gong, and Qiang Liu. Flow straight and fast: Learning to generate and
535 transfer data with rectified flow. *arXiv preprint arXiv:2209.03003*, 2022.

536

537 Yepeng Liu, Yiren Song, Hai Ci, Yu Zhang, Haofan Wang, Mike Zheng Shou, and Yuheng Bu.
538 Image watermarks are removable using controllable regeneration from clean noise. *arXiv preprint
arXiv:2410.05470*, 2024.

539

Rui Min, Sen Li, Hongyang Chen, and Minhao Cheng. A watermark-conditioned diffusion model
for ip protection. In *European Conference on Computer Vision*, pp. 104–120. Springer, 2024.

540 Ron Mokady, Amir Hertz, Kfir Aberman, Yael Pritch, and Daniel Cohen-Or. Null-text inversion for
 541 editing real images using guided diffusion models. In *Proceedings of the IEEE/CVF conference*
 542 *on computer vision and pattern recognition*, pp. 6038–6047, 2023.

543

544 Andreas Müller, Denis Lukovnikov, Jonas Thietke, Asja Fischer, and Erwin Quiring. Black-box
 545 forgery attacks on semantic watermarks for diffusion models. In *Proceedings of the Computer*
 546 *Vision and Pattern Recognition Conference*, pp. 20937–20946, 2025.

547

548 Minzhou Pan, Zhenting Wang, Xin Dong, Vikash Sehwag, Lingjuan Lyu, and Xue Lin. Finding
 549 needles in a haystack: A black-box approach to invisible watermark detection. In *European*
 550 *Conference on Computer Vision*, pp. 253–270. Springer, 2024a.

551

552 Yongyang Pan, Xiaohong Liu, Siqi Luo, Yi Xin, Xiao Guo, Xiaoming Liu, Xiongkuo Min, and
 553 Guangtao Zhai. Towards effective user attribution for latent diffusion models via watermark-
 554 informed blending. *arXiv preprint arXiv:2409.10958*, 2024b.

555

556 Ahmad Rezaei, Mohammad Akbari, Saeed Ranjbar Alvar, Arezou Fatemi, and Yong Zhang. Lawa:
 557 Using latent space for in-generation image watermarking. In *European Conference on Computer*
 558 *Vision*, pp. 118–136. Springer, 2024.

559

560 Robin Rombach, Andreas Blattmann, Dominik Lorenz, Patrick Esser, and Björn Ommer. High-
 561 resolution image synthesis with latent diffusion models. In *Proceedings of the IEEE/CVF confer-*
 562 *ence on computer vision and pattern recognition*, pp. 10684–10695, 2022.

563

564 Litu Rout, Yujia Chen, Nataniel Ruiz, Constantine Caramanis, Sanjay Shakkottai, and Wen-Sheng
 565 Chu. Semantic image inversion and editing using rectified stochastic differential equations. *arXiv*
 566 *preprint arXiv:2410.10792*, 2024.

567

568 Mehrdad Saberi, Vinu Sankar Sadasivan, Keivan Rezaei, Aounon Kumar, Atoosa Chegini, Wenxiao
 569 Wang, and Soheil Feizi. Robustness of ai-image detectors: Fundamental limits and practical
 570 attacks. *arXiv preprint arXiv:2310.00076*, 2023.

571

572 Qi Song, Ziyuan Luo, Ka Chun Cheung, Simon See, and Renjie Wan. Protecting nerfs’ copyright
 573 via plug-and-play watermarking base model. In *European Conference on Computer Vision*, pp.
 574 57–73. Springer, 2024.

575

576 Carl De Sousa Trias, Mihai Mitrea, Attilio Fiandrotti, Marco Cagnazzo, Sumanta Chaudhuri, and
 577 Enzo Tartaglione. Watermas: Sharpness-aware maximization for neural network watermarking.
 578 *arXiv preprint arXiv:2409.03902*, 2024.

579

580 Ved Umrajkar and Aakash Kumar Singh. Detection limits and statistical separability of tree
 581 ring watermarks in rectified flow-based text-to-image generation models. *arXiv preprint*
 582 *arXiv:2504.03850*, 2025.

583

584 Jiangshan Wang, Junfu Pu, Zhongang Qi, Jiayi Guo, Yue Ma, Nisha Huang, Yuxin Chen, Xiu Li,
 585 and Ying Shan. Taming rectified flow for inversion and editing. *arXiv preprint arXiv:2411.04746*,
 586 2024.

587

588 Yuxin Wen, John Kirchenbauer, Jonas Geiping, and Tom Goldstein. Tree-ring watermarks: Fin-
 589 gerprints for diffusion images that are invisible and robust. *arXiv preprint arXiv:2305.20030*,
 590 2023.

591

592 Xun Xian, Ganghua Wang, Xuan Bi, Jayanth Srinivasa, Ashish Kundu, Mingyi Hong, and Jie Ding.
 593 Raw: A robust and agile plug-and-play watermark framework for ai-generated images with prov-
 594 able guarantees. *Advances in Neural Information Processing Systems*, 37:132077–132105, 2024.

595

596 Yu Xu, Fan Tang, Juan Cao, Yuxin Zhang, Xiaoyu Kong, Jintao Li, Oliver Deussen, and Tong-Yee
 597 Lee. Headrouter: A training-free image editing framework for mm-dits by adaptively routing
 598 attention heads. *arXiv preprint arXiv:2411.15034*, 2024.

599

600 Pei Yang, Hai Ci, Yiren Song, and Mike Zheng Shou. Can simple averaging defeat modern water-
 601 marks? *Advances in Neural Information Processing Systems*, 37:56644–56673, 2024a.

594 Zijin Yang, Kai Zeng, Kejiang Chen, Han Fang, Weiming Zhang, and Nenghai Yu. Gaussian shad-
595 ing: Provable performance-lossless image watermarking for diffusion models. In *Proceedings*
596 *of the IEEE/CVF Conference on Computer Vision and Pattern Recognition*, pp. 12162–12171,
597 2024b.

598 Lijun Zhang, Xiao Liu, Antoni V Martin, Cindy X Bearfield, Yuriy Brun, and Hui Guan. Attack-
599 resilient image watermarking using stable diffusion. *Advances in Neural Information Processing*
600 *Systems*, 37:38480–38507, 2024a.

601 Yunming Zhang, Dengpan Ye, Sipeng Shen, and Jun Wang. Stylemark: A robust watermark-
602 ing method for art style images against black-box arbitrary style transfer. *arXiv preprint*
603 *arXiv:2412.07129*, 2024b.

604 Yunming Zhang, Dengpan Ye, Caiyun Xie, Long Tang, Xin Liao, Ziyi Liu, Chuanxi Chen, and
605 Jiacheng Deng. Dual defense: Adversarial, traceable, and invisible robust watermarking against
606 face swapping. *IEEE Transactions on Information Forensics and Security*, 19:4628–4641, 2024c.

607 Min Zhao, Fan Bao, Chongxuan Li, and Jun Zhu. Egsde: Unpaired image-to-image translation
608 via energy-guided stochastic differential equations. *Advances in Neural Information Processing*
609 *Systems*, 35:3609–3623, 2022.

610 Xuandong Zhao, Kexun Zhang, Zihao Su, Saastha Vasan, Ilya Grishchenko, Christopher Kruegel,
611 Giovanni Vigna, Yu-Xiang Wang, and Lei Li. Invisible image watermarks are provably removable
612 using generative ai. *Advances in neural information processing systems*, 37:8643–8672, 2024.

613
614
615
616
617
618
619
620
621
622
623
624
625
626
627
628
629
630
631
632
633
634
635
636
637
638
639
640
641
642
643
644
645
646
647